RATIONAL SELECTION OF EXPERIMENTAL DATA FOR INVERSE STRUCTURAL PROBLEMS

C. CHISARI[*], L. MACORINI[†], C. AMADIO[*] AND B.A. IZZUDDIN[†]

[*] Department of Engineering and Architecture
University of Trieste
Piazzale Europa, 1 34127 Trieste, Italy
e-mail: corrado.chisari@gmail.com, amadio@units.it

[†] Department of Civil and Environmental Engineering
Imperial College London
London SW7 2AZ, United Kingdom
email: l.macorini@imperial.ac.uk, b.izzuddin@imperial.ac.uk

Key Words: *Inverse problems, Proper Orthogonal Decomposition, Noise analysis, Measured data.*

Abstract. Inverse analysis has been established as an effective tool for parameter identification of physical models in many fields of civil engineering. One of the main issues in inverse analysis is defining the well-posedness of the problem when a limited set of data is considered. In fact as shown in previous work, the location and the number of the sensors providing the experimental data greatly affect the accuracy of the inverse procedure. In this paper it will be shown that, under certain circumstances, it is possible to approximate the global field as a linear combination of the experimental data. This provides a rational basis for the choice of the experimental equipment by minimising the effect of the measurement error on the solution of the inverse problem. A numerical application regarding the estimation of the main parameters of an advanced mesoscale model for masonry structures highlights the practicality of this study.

1 INTRODUCTION

Inverse analysis has been established as an effective tool for parameter identification of physical models in many fields of civil engineering [1], in industrial applications ([2], [3]) and for the solution of in-situ diagnostic problems ([4], [5], [6]).

In recent years, several methods for solving structural inverse problems have been proposed [7] but, as very often only a limited set of measured data is available, the minimization of the discrepancy function represents the most popular technique used in practical applications.

One of the main characteristics of inverse problems is that they can be severely ill-posed even when the corresponding forward problem is well-posed. According to Hadamard's

definition [8], an inverse problem is well-posed when i) the solution exists, ii) it is unique, and iii) it is stable, i.e. the solution of the "perturbed" problem remains in the neighbourhood of the "exact" solution also when a small noise is applied to the known terms. Moreover even if the existence and the uniqueness conditions hold, it is important to study the stability of the solution by accounting for noise effects, since they cannot be neglected when solving real problems.

An inverse problem may be ill-conditioned in a global sense or only for specific measurement data. In the first case, it is impossible to determine univocally the parameter vector by means of inverse techniques even when the full-field measurements are known. This means that the experimental setup has been poorly chosen, and the sensitivity of the response (in a global sense) to the variation of the input data is very low or null. However, even if the problem is globally well-posed, it may be possible that with the available experimental data, the sought parameters are strongly influenced by noise effects. Thus since type, number and location of the sensors used in the experimental tests are usually chosen in an empirical way, a rational methodology for the assessment of the experimental equipment is critical to exploit the full potential of the inverse procedure.

In this work, it will be shown that the use of finite element (FE) models allows the approximation of the global field as a function of a limited number of variables. If these are the measurable data, it is possible optimize their selection so as to control the propagation of the error from the measurements to the global field. Furthermore it will be shown that the global field obtained this way from the experimental data is strictly linked to the solution of the corresponding inverse problem, thus controlling the error in the "generated" global field means controlling the error of the inverse procedure in terms of material parameters. The "model reduction" is achieved by means of Proper Orthogonal Decomposition [9], while the choice of the sensor location can be seen as an optimisation problem, where the aim is minimising the effect of the noised data on the global response description. Hereinafter a practical application of the proposed approach is discussed. This corresponds to a numerical application where the main material parameters for a detailed mesoscale model for unreinforced masonry [10] are obtained from a simple test set-up. The application of inverse analysis techniques to this material model was investigated by the authors in previous research [6], where the need for an optimal set of experimental data was pointed out.

2 OVERVIEW OF THE ELASTIC INVERSE PROBLEM

Let us consider a mechanical system, of volume $\mathfrak{B}$ and boundary $\partial\mathfrak{B}$, defined by the position $\boldsymbol{x}$ in the reference configuration. It is known that the equations governing the quasi-static behaviour of the system are of three different types:

1. Equilibrium equations;
2. Compatibility equations;
3. Constitutive equations.

In direct (forward) problems, the aim is obtaining the vector field $\boldsymbol{u}$ and, consequently, the tensor field, by solving the system of Partial Differential Equations (PDEs) given by the above mentioned equations and the boundary conditions. The closed-form solution of such PDE system is known in very special cases; generally it can be approximated using a Finite Element discretization.

2

In inverse problems together with the previously mentioned unknowns, the constitutive parameters p, representative of the used material model, are to be sought. Clearly, the problem becomes under-determined, so some new conditions have to be added. These new conditions may be obtained from experimental measurements taken during the tests.

Let us suppose we have a mathematical model (or a FE model) $F(p, x)$ which, once the geometry, the spatial distribution of the material properties and the boundary conditions are known, gives the displacements as function of the material parameters p:

$$u(x) = F(p, x) \tag{1}$$

In the hypothetical case in which the full displacement field $\tilde{u}(x)$ is known, a necessary condition for the solution of the inverse problem is the equality between the computed and the reference fields,

$$F(p, x) = \tilde{u}(x) \ in \ \mathcal{B} \tag{2}$$

In globally well-posed inverse problems, this condition is also sufficient, and the most widely used method to solve inverse problems is the minimization of a "cost" function which measures the discrepancy between the measured data and the computed counterparts. With this approach, the optimization problem to be solved is:

$$p = \arg \min_{p} \left(\int_{\mathcal{B}} \|\tilde{u}(x) - F(p, x)\|^2 dV \right) \tag{3}$$

where $\|\cdot\|$ is a suitable norm measuring the discrepancy between the computed and the reference displacement.

Since Eqn. (2) is an overdetermined system, the solution is exact only in absence of noise in $\tilde{u}(x)$; otherwise it is a solution in a least-square sense and its quality depends on both the noise and the conditioning of the system.

The hypothesis of a whole displacement field being known is usually satisfied only for small specimens, restricting loading conditions (such as plane strain) and particular measurement equipment (i.e. Digital Imaging Correlation [11]). Conversely in most common cases, only a discrete number of displacement measurements is available which can be obtained using extensometers or trasducers (generically referred to as *sensors*). Thus it is critical to establish the amount of information carried by the experimental data, and how to select the optimal position for the sensors.

3   THE CASE OF A DISCRETE NUMBER OF EXPERIMENTAL DATA

When the full displacement field $\tilde{u}(x)$ is not known, and only a limited set of L data $\tilde{u}_i$ is available, it is common practice to replace the problem (3) with the following:

$$p = \arg \min_{p} \left(\sum_{i=1}^{L} \|\tilde{u}_i - F(p, x_i)\|^2 \right) \tag{4}$$

or, sometimes, with others having more complicated forms involving weight matrices and/or regularization terms. In Eqn. (4), x_i is the position of the i-th sensor.

While the solution of Eqn. (3) is the set p_1 which fits best the global experimental response, nothing is known about its relationship between the solution p_2 of (4), which only fits best the

data provided. It is intuitive that $\lim_{L\to+\infty} \boldsymbol{p_2} = \boldsymbol{p_1}$, but, for finite values of L, the discrepancy in the solution $\boldsymbol{p_2} - \boldsymbol{p_1}$ is not only function of L, but also of the position $\boldsymbol{x_i}$, and there is no guarantee that increasing the amount of data could improve the accuracy of the estimation (as proved in [12] with reference to an inverse problem of gravity). In the next subsection, the relationship between the displacement field and a discrete number of data is investigated.

3.1 From a displacement field to discrete values

Using the Finite Element Method the domain can be discretised into finite number of elements and the dependency of $\boldsymbol{u}$ on the position $\boldsymbol{x}$ in the global reference system can be made explicit by means of the relationship:

$$\boldsymbol{u} = \boldsymbol{F}(\boldsymbol{p}, \boldsymbol{x}) = \boldsymbol{B_u}(\boldsymbol{x_e}) \, \boldsymbol{A_e} \, \boldsymbol{U}(\boldsymbol{p}) \tag{5}$$

in which the subscript e indicates the element which the point P with global and local coordinates $\boldsymbol{x}$ and $\boldsymbol{x_e}$, belongs to. The matrix $\boldsymbol{B}(\boldsymbol{x_e})$ collects the *shape functions*, which depend on the type of finite element considered. The transformation matrix $\boldsymbol{A_e}$ transforms the global nodal displacement vector $\boldsymbol{U}$ into the local reference system. Since the shape functions and the transformation matrix are known a priori, the dependence of the full displacement field on the material parameters is completely characterized by the knowledge of the relationship $\boldsymbol{U} = \boldsymbol{U}(\boldsymbol{p})$. From a theoretical point of view, imposing the equality between the displacement field (functional equality (2)) is equivalent to imposing the vectorial equality:

$$\boldsymbol{U}(\boldsymbol{p}) = \widetilde{\boldsymbol{U}} \tag{6}$$

where $\widetilde{\boldsymbol{U}}$ is the N-sized vector collecting the displacements of the nodes in which the structure is discretised. If we neglect the possible error given by the used shape functions, the inverse problem is solved when a limited number of displacements i.e. the nodal displacements are known, and the infinite-sized system (2) is replaced by the N-sized system (6).

In most cases, the choice of the nodal discretisation for the analysed domain is clearly distinct from the choice of the nodes the displacements of which are recorded during the test and usually N is much larger than L. What we want to prove, though, is that, once L displacements $\widetilde{\boldsymbol{u}_i}$ are available, it is possible to express the vector $\widetilde{\boldsymbol{U}}$ as linear combination of them.

Let us suppose that it is possible to exploit the dependence of $\boldsymbol{U}$ on $\boldsymbol{p}$ by simply choosing a convenient basis. In this work, the choice of the new basis has been done by analysing the behaviour of the structure using Proper Orthogonal Decomposition (POD, [9]) and varying $\boldsymbol{p}$ randomly. Thus the displacement field expressed in the new basis reads:

$$\boldsymbol{U}(\boldsymbol{p}) = \sum_{i=1}^{K} a_i(\boldsymbol{p}) \, \boldsymbol{\varphi_i} = \boldsymbol{\Phi} \, \boldsymbol{a}(\boldsymbol{p}) \tag{7}$$

where $\boldsymbol{\Phi}$ is an $N \times K$ matrix representing the new basis and $\boldsymbol{a(p)}$ is a vector collecting K amplitudes. This way, the dependence on $\boldsymbol{p}$ is restricted to the amplitudes, while the basis is fixed once-for-all. If $K=N$, $\boldsymbol{U}$ is simply expressed in a different equivalent basis. On the other hand if the variation of the material parameters $\boldsymbol{p}$ acts on $\boldsymbol{U}$ simply modifying the relative importance of a limited number $K<<N$ of "shapes" $\boldsymbol{\varphi_i}$, the advantages in expressing $\boldsymbol{U}$ as in (7) become apparent.

In fact let us consider a displacement u_i. From (7), it can be written as:

$$u_i = \Phi^i\, a(p) \tag{8}$$

where Φ^i is the $3 \times K$ matrix obtained choosing the rows of Φ corresponding to the displacements u_i. Consequently, the vector u collecting the L displacements u_i can be expressed as:

$$u = \Phi_r\, a(p) \tag{9}$$

with:

$$\Phi_r = \begin{bmatrix} \Phi^1 \\ ... \\ \Phi^L \end{bmatrix} \tag{10}$$

On the other hand, a relative displacement Δu^k between two points (respectively placed at $x^{k,1}$ and $x^{k,2}$) along the direction of the line connecting them (i.e. as in the case of relative displacements measured by transducers in physical tests) can be expressed as:

$$\Delta u^k = \left(u^{k,2} - u^{k,1}\right)^T c_k = c_k{}^T\left(\Phi^{k,2} - \Phi^{k,1}\right) a \tag{11}$$

where c_k is the vector of the director cosines of the direction considered. The matrix Φ_r now becomes:

$$\Phi_r = \begin{bmatrix} c_1{}^T(\Phi^{1,2} - \Phi^{1,1}) \\ ... \\ c_L{}^T(\Phi^{L,2} - \Phi^{L,1}) \end{bmatrix} \tag{12}$$

If rank(Φ_r)=K, it is possible to invert eqn. (9) obtaining:

$$a = \Phi_r{}^\dagger\, u \tag{13}$$

where $\Phi_r{}^\dagger$ is the left pseudo-inverse matrix of Φ_r ($\Phi_r{}^\dagger = \Phi_r{}^{-1}$ if Φ_r is squared). From (7) and (13):

$$U = \Phi\, \Phi_r{}^\dagger\, u = P\, u \tag{14}$$

3.2 The choice of the sensors

Expression (14) is a linear relationship between the nodal displacement vector and a limited set of data (both absolute displacements, eqn. (10), or relative displacements, eqn. (12)). Thus it is natural to investigate how an error in u propagates into the global response. Applying a perturbation to u in Eqn. (14) and subtracting the unperturbed expression it can be obtained:

$$\delta U = P\, \delta u \tag{15}$$

Reminding one of the basic equations for the norm of a matrix:

$$\|\delta U\| \le \|P\|\, \|\delta u\| \tag{16}$$

it is clear that given an error in the measured data u (usually not controllable), an upper bound for the error in the vector U (and, consequently, in the global field) is given by the norm of the matrix P. Since P changes with changing sensor locations X (through the terms of

$\Phi_r{}^\dagger$), a rational approach in the choice of the measurement data may be the minimization of the corresponding norm $\|P\|$:

$$X_s = \begin{bmatrix} x_{s1} \\ \cdots \\ x_{sL} \end{bmatrix} = \arg \min_X (\|P(X)\|) \tag{17}$$

where x_{si} indicates the position of the i-th sensor. Although difficult to express in an analytical form, the optimization problem (17) can be easily treated by using meta-heuristic techniques such as Genetic Algorithms [13].

It is important to point out that there is an implicit relationship between the global field evaluated in (14) and the solution of (4). In fact, neglecting the error made in the compact representation (7), the displacements U are obtained by solving the overdetermined system (9) using a least-square approach. This represents the global displacement field whose nodal displacement u fits best the experimental data among all possible representations given by the FE model. On the other hand, that is the same definition for the solution of (4), which corresponds to the vector p giving the best fitting nodal displacements $F(p, x_i)$ in a least-square sense. It results that the solution of the inverse problem will be as accurate as $U = P u$ and the propagation of the error in the inverse procedure can be easily controlled by a careful choice of the sensor location.

4 A NUMERICAL APPLICATION

In this numerical application the main elastic material parameters of an advanced mesoscale model [10] for masonry structures are obtained utilising inverse analysis techniques. After a brief description of both the material model and the FE description for a specific experimental setup, the influence of random errors in the displacement field on the solution of the inverse problem is analysed. With this aim a "pseudo-experimental" approach is used and a vector p is fixed a priori, while the displacements are evaluated performing FE analysis eventually perturbed by a random noise. The comparison between the solution of the "perturbed" inverse problem and the known solution allows an accurate investigation of the noise effects.

4.1 The material model

In the mesoscale model employed here to represent brick/block-masonry [10], blocks are modelled using continuous 20-noded elastic solid elements whereas mortar and the brick–mortar interfaces are modelled by means of 16-noded 2D nonlinear interface elements. The interface local material model is formulated in terms of one normal and two tangential tractions σ and relative displacements u evaluated for each integration point over the reference mid-plane. In the elastic range, they are linked by the expression:

$$\sigma = k_0 u \qquad \begin{Bmatrix} \tau_x \\ \tau_y \\ \sigma \end{Bmatrix} = \begin{bmatrix} k_V & 0 & 0 \\ 0 & k_V & 0 \\ 0 & 0 & k_N \end{bmatrix} \begin{Bmatrix} u_x \\ u_y \\ u_z \end{Bmatrix} \tag{18}$$

in which specific elastic stiffness values are considered assuming decoupling of the normal k_N and tangential k_V stiffness. In the following the unknowns are represented by the vector

6

$\boldsymbol{p} = \begin{bmatrix} k_V \\ k_N \end{bmatrix}$, while brick Young modulus is assumed to be known. Zero-thickness interfaces are also arranged in the vertical mid-plane of all blocks, but in this work their stiffness is set very high to model the continuity of the material. This material model was previously developed and implemented into ADAPTIC, a general finite element code [14].

4.2 The experimental test

The experimental test analysed in this work is a compressive diagonal test on an approximately squared masonry panel. It is widely used in practise ([15], [16]) to estimate strength of masonry as a homogeneous material. In this paper it will be shown that this test can provide also useful information to obtain the elastic properties of interface elements representing mortar joints when using the previously described mesoscale model.

The experimental setup is shown in **Figure 1**-a. A $1170 \times 1200 \times 120$ mm^3 large masonry panel, made up of $250 \times 60 \times 120$ mm^3 large bricks and 10 mm thick mortar joints is subjected to an imposed diagonal displacement $u_d = 1$ mm. The structure is assumed to behave elastically. The pseudo-experimental model is created imposing $k_V = 50$ N/mm^3, $k_N = 120$ N/mm^3, $E_b = 2500$ N/mm^2, $\nu = 0.15$, where k_V and k_N are the mortar interface stiffness values described in section 4.1, and E_b and ν are the brick Young modulus and Poisson ratio, respectively. The displacement field of the pseudo-experimental model is shown in **Figure 1**-b.

(a)   (b)
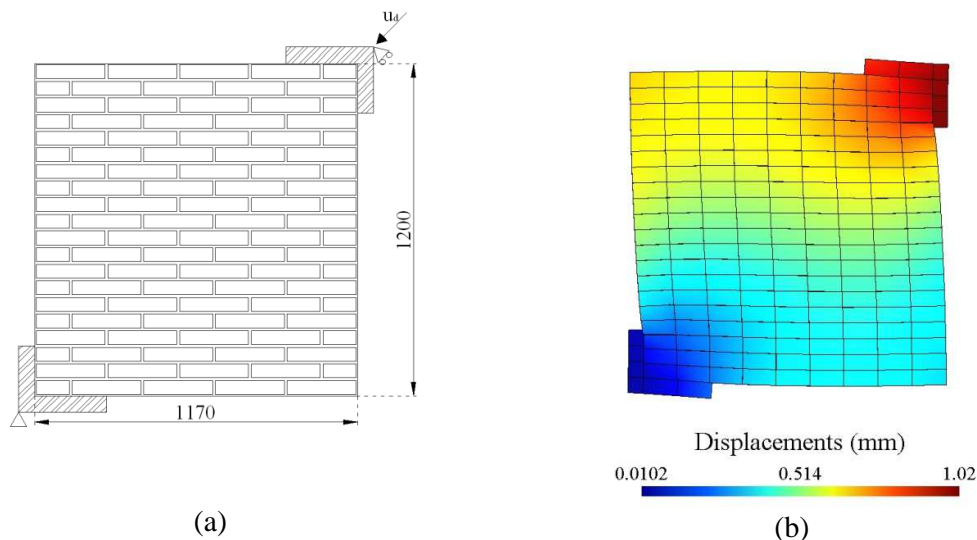
Figure 1: (a) Experimental setup and (b) pseudo-experimental displacement field.

4.3 The POD analysis

To create the POD basis, 200 FE model samples with variable material parameters $\boldsymbol{p}$ have been considered. The samples have been generated by varying $\boldsymbol{p}$ in a reasonable range (**Table 1**) by using a pseudo-random technique (i.e. Sobol sequence [17]).

Table 1: Variation range of the interface elastic stiffnesses

Parameter	Lower bound (N/mm^3)	Upper bound (N/mm^3)	Step (N/mm^3)
k_V	10	300	1
k_N	30	500	1

In the POD theory, it is possible to prove that the error in the POD approximation is controlled by the ratio:

$$r = \frac{\sum_{i=1}^{K} \lambda_i}{\sum_{i=1}^{M} \lambda_i} \qquad (19)$$

with:

- K number of chosen modes;
- M number of samples
- λ_i i-th eigenvalue of the modified correlation matrix $\boldsymbol{D} = \boldsymbol{U^T U}$. $\boldsymbol{U}$ is the so-called *snapshot* matrix, i.e. the matrix collecting the displacements of the samples as columns.

The analysis shows that 3 modes are sufficient to approximate the response, as they provide $r \cong 100\%$. A graphical representation of the three modes is shown in **Figure 2**.
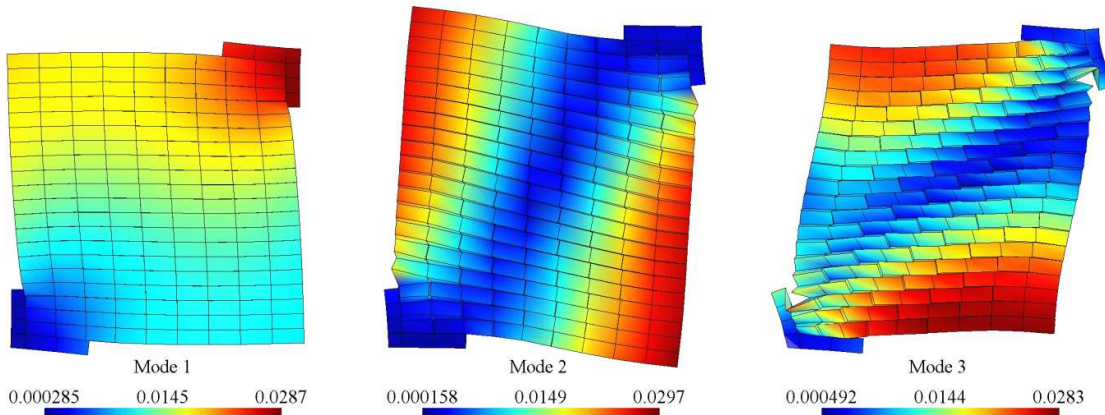
Figure 2: Basic modes after the POD analysis.

4.4 Error propagation analysis

In the analysis different measurement setups are considered: i) setup 1 - the whole nodal displacement vector $\boldsymbol{U}$; ii) setup 2 -nine sensors measuring relative displacements in the vertical direction **Figure 13**-a; iii) setup 3 - nine sensors placed as the outcomes of the optimization problem given by eqn. (17) and solved by a Genetic Algorithm **Figure 13**-b. This is not described here for the sake of briefness.
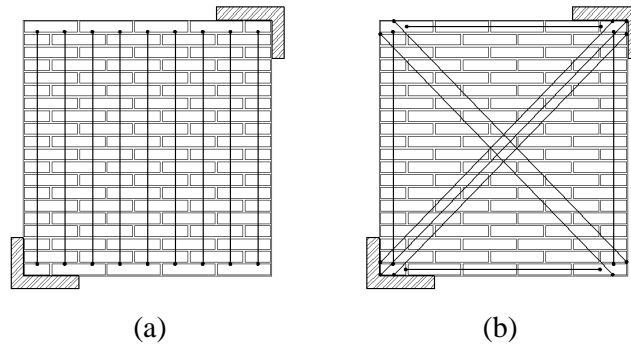
Figure 3: (a) Sensor setup 2 and (b) setup 3.

A uniform random noise of amplitude $\pm 0.01\,mm$ has been applied to the pseudo-experimental displacement field. By means of Eqn. (14) it is possible to evaluate the "best fitting" displacement field, given the set of data provided by the three measurement setups, and compare it with the "real" field shown in **Figure 1**-b. The results are reported in **Figure 4**.

Some considerations may be done. The knowledge of the overall perturbed displacement field allows for the determination of an error-averaged field which is affected by a remarkable less inaccuracy. Expression (14) represents a sort of "regularization" of the field, averaging the error. In the "regularized" version of the field (**Figure 4**-b), the maximum error (0.00257 mm) is about six times smaller than the maximum in the original perturbed field (0.0167 mm, see **Figure 4**-a). As far as sensor setup 2 is concerned, it is greatly affected by the error in the measurements (maximum error in the generated field equal to 0.255 mm). On the contrary, a rational arrangement of the nine sensors (setup 3) allows for a minimal propagation of the error onto the generated field (maximum error 0.00677 mm).

The Frobenius norm of the matrix $\boldsymbol{P}$ (Eqn. (16)), which is an upper bound to the perturbation of the generated field, as shown in section 3.2, reflects these considerations. In fact for the proposed setups we have:

- $\|P\|_{F,1} = \sqrt{K} = 1.732$
- $\|P\|_{F,2} = 1239.2$
- $\|P\|_{F,3} = 37.36$

9
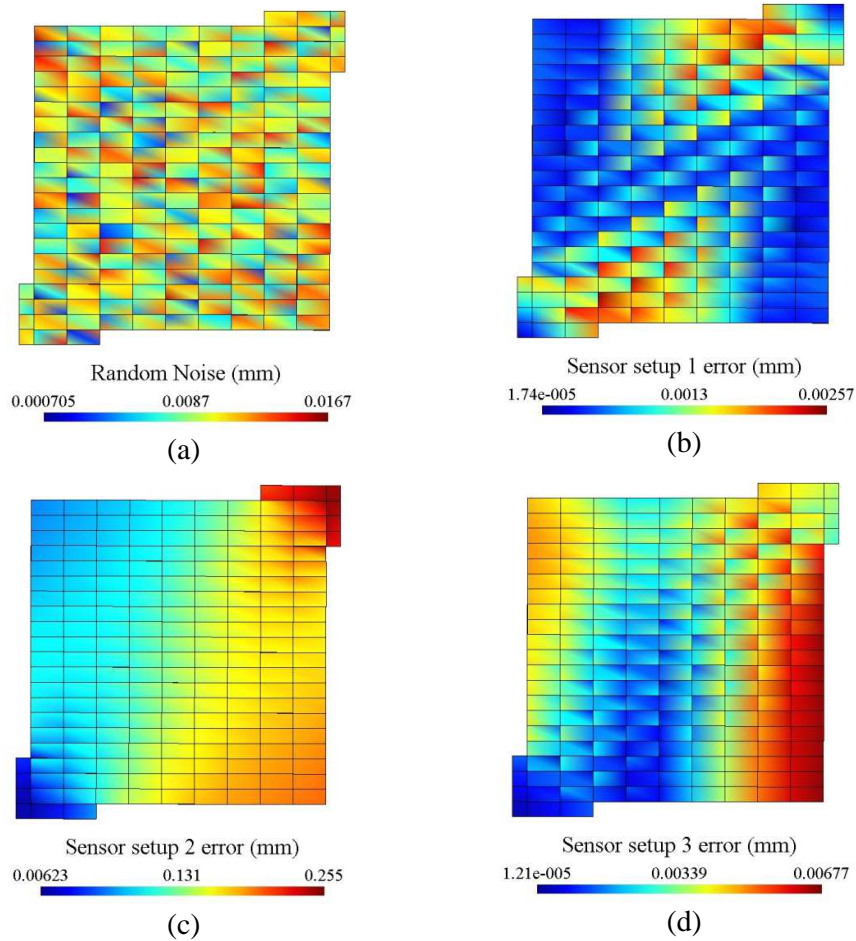
Figure 4: (a) Random noise, (b) "best fitting" displacement field for sensor setup 1, (c) setup 2 and (d) setup 3.

4.5 The inverse analysis

Inverse analysis has been carried out assessing the ability of the sensor setups described in the previous section to solve the calibration problem for the elastic interface stiffness values. 30 perturbations of the pseudo-experimental displacement field (in the range $\pm 0.01 \, mm$) have been considered, and each of them has been assumed as known term in the discrepancy function (4) for the sensor setup 1. Furthermore for each perturbation, the nine relative displacements corresponding to the nine sensors of setups 2 and 3 have been evaluated. They thus represent the variables $\tilde{u}_i$ in (4), and $L = 9$ in these cases. The minimization of the discrepancy function has been carried out by means of the Genetic Algorithm described in [6]. The results are shown in **Figure 5**.

10

(a)　　　　　　　　　　　(b)　　　　　　　　　　　(c)
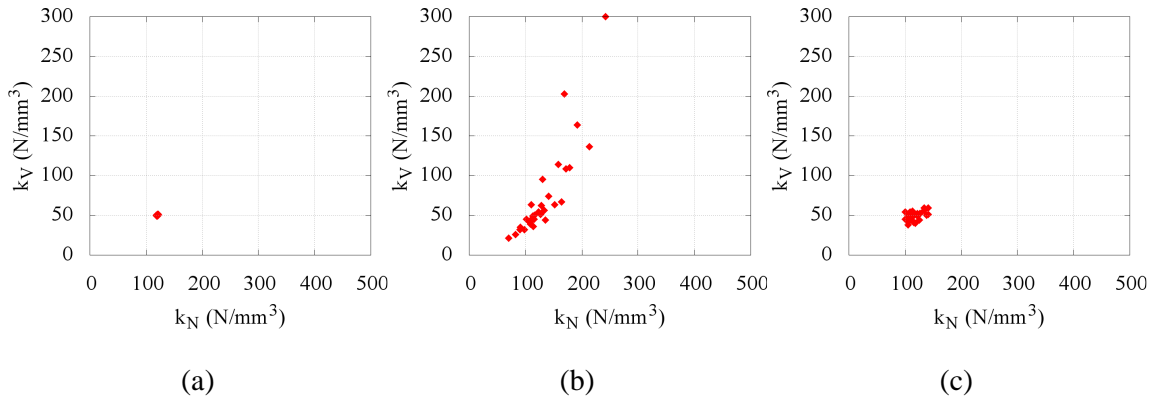
Figure 5: Results of the inverse analyses with sensor setup 1 (a), 2 (b) and 3 (c).

The global well-posedness of the problem is confirmed by the excellent results obtained using the whole displacement field (sensor setup 1, **Figure 5**-a), where it is clear that the knowledge of the field allows an accurate estimation of the material parameters even in presence of a random noise. On the other hand, the inverse analysis reflects the inadequacy of the sensor setup 2 when compared against sensor setup 3. The error in the parameter estimation is practically unbound in the first case, while very limited in the other one. It confirms what has been said about the representativeness of the measured data with respect to the global field, and, as consequence, the well-posedness of the inverse problem when a limited set of experimental data is available.

5   CONCLUSIONS

In this work a numerical study has been carried out to investigate the well-posedness of elastic inverse problems when different sets of experimental data are considered. It has been shown that it is possible to approximate the global displacement field as a linear combination of the experimental data. Furthermore, the displacement field obtained this way from noise-affected data is strictly related to the solution of the inverse problem when the same data are used in the minimisation of a discrepancy function. Thus it has been found that a rational basis for the optimal experimental equipment (number and location of the sensors) for the inverse problem can be based on the control of the propagation of the error from the measured data to the global field. The application of the proposed procedure to a simple laboratory test on a masonry specimen modelled by means of a mesoscale description confirms that a proper choice of the experimental equipment is crucial to maintain the well-posedness of the global problem.

11

REFERENCES

[1]. Stavroulakis, G.E., Bolzon, G., Waszczyszyn, Z., Ziemianski, L. Inverse Analysis. *Comprehensive Structural Integrity* (2003), Elsevier Publishers. Chapter 3, pp. 685-718.

[2]. Ageno, M., Bolzon, G., Maier, G. An inverse analysis procedure for the material parameter identification of elastic–plastic free-standing foils. *Struct Multidisc Optim* (2009) **38**:229–243.

[3]. Bocciarelli, M., Maier, G. Indentation and imprint mapping method for identification of residual stresses. *Computational Materials Science* (2007) **39**:381–392.

[4]. Ardito, R., Maier, G., Massalongo, G. Diagnostic analysis of concrete dams based on seasonal hydrostatic loading. *Engineering Structures* (2008) **30**:3176–3185.

[5]. Fedele, R., Maier, G., Miller, B. Health assessment of concrete dams by overall inverse analyses and neural networks. *International Journal of Fracture* (2006) **137**:151–172.

[6]. Chisari, C., Macorini, L., Amadio, C., Izzuddin, B.A. Identification of Brick-Masonry Material Properties Through Inverse Analysis and Genetic Algorithms. *Proceedings of the Fourteenth International Conference on Civil, Structural and Environmental Engineering Computing* (2013), Civil-Comp Press, Stirlingshire, UK, Paper 70.

[7]. Avril, S., Bonnet, M., Bretelle, A.-S., Grédiac, M., Hild, F., Ienny, P., Latourte, F., Lemosse, D., Pagano, S., Pagnacco, E., Pierron, F. Overview of identification methods of mechanical parameters based on full-field measurements. *Experimental Mechanics* (2008) **48**(4):381-402.

[8]. Kabanikhin, S.I. Definitions and examples of inverse and ill-posed problems. *J. Inv. Ill-Posed Problems* (2008) **16**:317-357.

[9]. Liang, Y.C., Lee, H.P., Lim, S.P., Lee, K.H., Lin, W.Z. Proper Orthogonal Decomposition and its applications — part i: theory. *J Sound Vibration* (2002) **252**(3): 527–544.

[10]. Macorini, L., Izzuddin, B.A. A non-linear interface element for 3D mesoscale analysis of brick-masonry structures. *Int. J. Numer. Meth. Engrg.*, (2011) **85**:1584-1608.

[11]. Hild, F., Roux, S. Digital Image Correlation: from Displacement Measurement to Identification of Elastic Properties - a Review. *Strain* (2006) **42**:69-80.

[12]. Balk, P.I. A priori information and admissible complexity of the model of anomalous objects in the solution of inverse problems of gravity. *Izvestiya, Physics of the Solid Earth* (2013) **49**(2): 165-176.

[13]. Goldberg, D.E. *Genetic algorithms in search, optimization and machine learning,* Addison-Wesley (1989).

[14]. Izzuddin, B.A. *Nonlinear dynamic analysis of framed structures*, Ph.D Thesis, Imperial College, London, 1991.

[15]. Corradi, M., Borri, A., Vignoli, A. Experimental study on the determination of strength of masonry walls. *Construction and Building Materials* (2003) **17**:325–337.

[16]. Milosevic, J., Gago, A.S., Lopes, M., Bento, R. Experimental assessment of shear strength parameters on rubble stone masonry specimens. *Construction and Building Materials* (2013) **47**:1372-1380.

[17]. Antonov, I.A., Saleev, V.M. An economic method of computing LP tau-sequence. *USSR Computational Mathematics and Mathematical Physics* (1979) **19**(1):252-256.

12